

# The Proximity of Mercury's Spin to Cassini State 1

S. J. Peale

*Department of Physics  
University of California  
Santa Barbara, CA 93106  
peale@io.physics.ucsb.edu*

## ABSTRACT

In determining Mercury's core structure from its rotational properties, the value of the normalized moment of inertia,  $C/MR^2$ , from the location of Cassini 1 is crucial. If Mercury's spin axis occupies Cassini state 1, its position defines the location of the state, where the axis is fixed in the frame precessing with the orbit. Although tidal and core-mantle dissipation drive the spin to the Cassini state with a time scale  $O(10^5)$  years, the spin might still be displaced from the Cassini state if the variations in the orbital elements induced by planetary perturbations, which change the position of the Cassini state, cause the spin to lag behind as it attempts to follow the state. After being brought to the state by dissipative processes, the spin axis is expected to follow the Cassini state for orbit variations with time scales long compared to the 1000 year precession period of the spin about the Cassini state because the solid angle swept out by the spin axis as it precesses is an adiabatic invariant. Short period variations in the orbital elements of small amplitude should cause displacements that are commensurate with the amplitudes of the short period terms. The exception would be if there are forcing terms in the perturbations that are nearly resonant with the 1000 year precession period. The precision of the radar and eventual spacecraft measurements of the position of Mercury's spin axis warrants a check on the likely proximity of the spin axis to the Cassini state. How confident should we be that the spin axis position defines the Cassini state sufficiently well for a precise determination of  $C/MR^2$ ?

By following simultaneously the spin position and the Cassini state position during long time scale orbital variations over past 3 million years (Quinn *et al.*, 1991) and short time scale variations for 20000 years (JPL Ephemeris DE 408, E. M. Standish, private communication, 2005), we show that the spin axis will remain within one arcsec of the Cassini state after it is brought there by dissipative torques. In this process the spin is located in the orbit frame of reference, which in turn is referenced to the inertial ecliptic plane of J2000. There are no perturbations with periods resonant with the precession period that could cause large separations. We thus expect Mercury's spin to occupy Cassini state 1 well

within the uncertainties for both radar and spacecraft measurements, with correspondingly tight constraints on  $C/MR^2$  and the extent of Mercury’s molten core. Two unlikely caveats for this conclusion are 1. an excitation of a free spin precession by an unknown mechanism or 2. a displacement by a dissipative core mantle interaction that exceeds the measurement uncertainties.

## 1. Introduction

Radar observations have begun the process of determining the extent of Mercury’s molten core (Margot et al. 2003), and the experiment will be completed when the MESSENGER spacecraft orbits Mercury in 2011 (Solomon et al. 2001). The BepiColombo spacecraft will complement and augment the observations of MESSENGER, but will orbit Mercury sometime after 2011 (Anselmi and Scoon, 2001). The experiment is based on the product of three factors (Peale, 1976; 1981; 1988; 2005; Peale et al. 2002).

$$\left(\frac{C_m}{B-A}\right)\left(\frac{MR^2}{C}\right)\left(\frac{B-A}{MR^2}\right) = \frac{C_m}{C} \leq 1, \quad (1)$$

where  $A < B < C$  are the principal moments of inertia of Mercury with  $C_m$  being the polar moment of inertia of the mantle alone, and  $M$  and  $R$  are Mercury’s mass and radius respectively. The first factor is determined by the amplitude of the physical libration,  $\phi_0 = [3(B-A)/2C_m](1 - 11e^2 + \dots)$ , where  $e$  is the orbital eccentricity and  $C_m$  appears in the denominator because the liquid core is not expected to follow the mantle during the short period librations (Peale, et al. 2002). The second factor follows from the analysis of generalized Cassini’s laws for Mercury (Colombo, 1966; Peale, 1969; Beletskii, 1972) (see Section 3).

$$\frac{C}{MR^2} = \frac{nJ_2}{w_L} \frac{f(e)}{(\sin I')/i_c + \cos I'}, \quad (2)$$

where  $f(e) = G_{210}(e) + 2C_{22}G_{201}(e)/J_2$ ,  $n = \sqrt{GM_\odot/a^3}$  is the orbital mean motion, ( $G$  is the gravitational constant,  $M_\odot$  is the solar mass,  $a$  is the semimajor axis of the orbit), the functions  $G_{210}(e) = (1 - e^2)^{-3/2}$  and  $G_{201}(e) = 7e/2 - 123e^3/16 + \dots$  are defined by Kaula (1966),  $J_2$  and  $C_{22}$  are the second degree coefficients in the expansion of Mercury’s gravitational field,  $I'$  is the inclination of the orbit plane to the Laplace plane, the plane on which Mercury’s orbit precesses with nearly constant inclination and at a nearly constant rate whose magnitude is  $w_L$ , and  $i_c$  is the obliquity of the Cassini state. The orientation of the Laplace plane and the value of  $w_L$  are determined by averaging the orbital element variations over a suitable time interval as discussed below. The last factor is found from  $C_{22} = (B - A)/(4MR^2)$ .

Fig. 1 shows the geometry of Cassini state 1 for Mercury, where Mercury’s obliquity  $i = i_c$  with the ascending nodes of the equator plane on the orbit plane and of the orbit plane on the Laplace plane remaining coincident as the spin and orbit normal precess around the normal to

the Laplace plane. The Laplace plane is determined mainly by Venus, Earth and Jupiter as is the precession of Mercury’s orbit. Because of the orbit precession, the spin precesses around the Cassini state and tends toward that state from dissipative effects rather than toward the orbit normal (Peale, 1974; Ward, 1975).

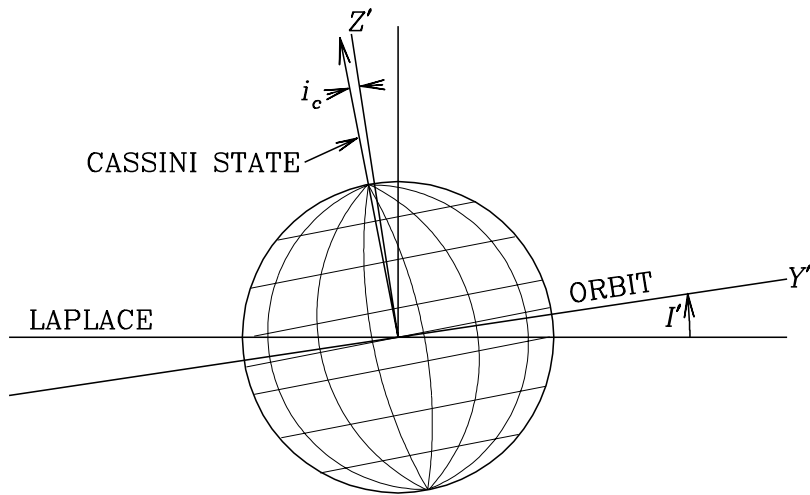


Fig. 1.— Geometry of Cassini state 1. The ascending node of the equator on the orbit plane and the ascending node of the orbit on the Laplace plane remain coincident as they precess around the normal to the Laplace plane at the current rate corresponding to the orbit precession period of about 300,000 years.

The determination of  $\phi_0$ ,  $J_2$ ,  $C_{22}$ , and  $i_c$  thus yields  $C_m/C$ . Empirical constraints on  $C/MR^2$  must wait for MESSENGER determinations while in orbit. Crucial to the determination of moment of inertia is the assumption that the spin axis occupies Cassini state 1 (Eq. (2)). Only if we are confident that the measured obliquity  $i = i_c$ , can we constrain the value of  $C/MR^2$  with sufficient precision to determine the extent of Mercury’s liquid core. Knowing the internal structure of Mercury is important for inferring the thermal history, overall chemical composition and the constraints Mercury can place on the details of origin and evolution of the terrestrial planets (Harder and Schubert, 2001; Solomon et al. 2001).

Tidal friction will drive Mercury’s spin to Cassini state 1 from virtually any initial obliquity (Peale, 1974; Ward, 1975), and the addition of dissipation between a liquid core and solid mantle will hasten that evolution, provided the initial obliquity  $i < 90^\circ$ , with a time scale from both tides and core-mantle dissipation together of order  $10^5$  years (Peale, 2005). As Mercury’s spin axis approaches the Cassini state, it will precess around that state with a period near 500 or 1000 years depending on whether or not the liquid core is dragged along with the spin precession. A finite amplitude free precession would frustrate the determination of  $i_c$ , but the short time scale for its decay makes a remnant free spin precession unlikely, unless there is a recent, unspecified excitation mechanism (Peale, 2005).

Another possibility for a displacement of the spin from the Cassini state is if the spin is unable to follow the Cassini state sufficiently closely as the position of the state changes due to the variations in the orbital elements and Laplace plane orientation from planetary perturbations and changing solar system geometry. We can expect the spin to remain reasonably close to the Cassini state after being brought there by dissipative processes because the following action integral is an adiabatic invariant, where the integral is nearly constant if the period of the angle variable is short compared to all other relevant time scales (Goldreich and Toomre, 1969; Peale, 1974).

$$\oint p' dq' = -\alpha \oint (1 - \cos \theta') d\phi' \approx \text{const}, \quad (3)$$

where the action variable  $p' = -\alpha(1 - \cos \theta')$  with  $\alpha$  being the spin angular momentum, and  $q' = \phi'$  is the angle variable, with  $\theta'$  and  $\phi'$  being the ordinary spherical polar coordinates of the spin vector in the system with the  $Z$  axis aligned with the Cassini state. That  $p'$  and  $q'$  are conjugate variables is verified by  $dp'/dt = -\partial H/\partial q'$  and  $dq'/dt = \partial H/\partial p'$ , with  $H$  being the Hamiltonian for the Mercury’s rotational dynamics written in the frame precessing with the orbit (Peale, 1974). The action integral is seen to be  $-\alpha$  times the solid angle contained by the spin vector as it precesses around the Cassini state, and it is approximately conserved if the spin precession rate  $\dot{\phi}'$  is fast relative to the significant changes in the parameters determining the position of the state. The angle variable describes the precession of the spin about the Cassini state. We shall see below that the large amplitude variations in the orbital parameters relative to the ecliptic plane have periods exceeding  $5 \times 10^4$  years, which is sufficiently long compared to the 1000 year precession period that one expects the adiabatic invariant to keep the spin close to the current position of the Cassini state (once it is there) as the latter’s position changes slowly on these time scales. The adiabatic invariant is not conserved on the time scale of short period variations, but these variations are of small amplitude, and we shall see that the spin follows the Cassini state defined by the orbital elements averaged in a 2000 year window over the 20,000 year JPL Ephemeris DE 408. The precision of the radar determinations of Mercury’s spin properties, and that anticipated for the MESSENGER and BepiColombo missions warrants a check on just how well the spin axis follows the Cassini state for all variations of the parameters defining the state.

Our purpose here is to develop a formalism to test how close to the Cassini state the spin axis remains for both slow and fast variations in the orbital parameters. We shall consider the variations of  $e$ ,  $I$ ,  $\Omega$ , and their derivatives due to the planetary perturbations, where  $I$  and  $\Omega$  are the orbit inclination and longitude of the ascending node of the orbit on the ecliptic plane respectively. Dissipative processes will relentlessly drive the spin to the Cassini state, so the test will determine how closely Mercury’s spin axis follows the Cassini state position as the position of the state changes due to the orbital element variations. To this end we develop the equations of motion of Mercury’s spin vector relative to the orbit frame of reference, averaged over an orbit period, in Section 2, and find the position of the spin and the position of the Cassini state as a function of time as variations in the orbital parameters ensue. Finding the Cassini state position will involve defining a set of coplanar vectors that includes the normal to the Laplace plane. The inclination of the orbit relative to the Laplace plane and the rate of precession of the ascending node of the orbit on the Laplace plane do not have to be known with high precision to define the position of the Cassini state accurately (Yseboodt and Margot, 2005). For the slow variations in  $e$ ,  $I$ ,  $\Omega$ ,  $dI/dt$  and  $d\Omega/dt$ , we shall vary the orbital elements and their time derivatives according to simulations by T. Quinn (Quinn et al. 1991) over the past  $3 \times 10^6$  years.<sup>1</sup> For the short period variations in the orbital elements we follow the spin and Cassini state positions as  $e$ ,  $I$ ,  $\Omega$ ,  $dI/dt$  and  $d\Omega/dt$  vary according to the 20,000 year JPL Ephemeris DE 408 provided by Myles Standish, but now the Cassini state position will be determined by elements and rates averaged over the 2000 year window mentioned above. Periodic variations of the same variables with amplitudes and periods representative of the true variations are also applied to identify the sources of the fluctuations in the spin-Cassini state separation that are observed.

In Section 3 we determine the time varying position of the Cassini state, where variations in  $dI/dt$  and  $d\Omega/dt$  change the Laplace plane orientation and the variations in  $I$ ,  $e$  and  $w$  change  $i_c$ . This determination allows us to compare the position of the spin vector with the Cassini state position at any time. All dissipative forces are ignored, and principal axis rotation is assumed. The neglect of dissipation means we couple the liquid core firmly to the mantle, which is equivalent to Mercury’s having a solid core. Consequences of the relaxation of this latter assumption will be pursued in a later paper.

In Section 4, the spin vector, placed initially in the Cassini state, is shown to remain within approximately  $1''$  of the Cassini state position as this position is continuously redefined for the continuously varying Laplace plane and orbital elements as given over the past  $3 \times 10^6$  years by the Quinn simulation. Equivalently, the spin vector would maintain any small initial separation from the Cassini state to within  $1''$ . The effect of higher frequency terms on the spin-Cassini state separation is found in Section 5. Large separations of the spin from the Cassini state are forced for periodic variations in the inclination with periods near the spin

---

<sup>1</sup><ftp://ftp.astro.washington.edu/pub/hpcc/QTD>

precession period. However, any terms with periods near resonance with the spin precession period are not evident in the real variations of  $e$ ,  $I$ ,  $\Omega$ ,  $dI/dt$  and  $d\Omega/dt$ . This is demonstrated by the spin and Cassini state positions (from locally averaged values of elements and rates) remaining within 1" for variations of these parameters given by JPL Ephemeris DE 408. A summary and discussion follows in Section 6, where we end with a conjecture on the possible effect of the liquid core on the position of the spin axis.

## 2. Equations of variation

Fig. 2 defines the coordinate systems centered on Mercury to be used along with some of the variables. The  $XYZ$  system is the inertial ecliptic plane of J2000 with the  $Z$  axis perpendicular to the plane. The  $X'Y'Z'$  system has the  $Z'$  axis perpendicular to the orbit plane and the  $X'$  axis along the ascending node of the orbit plane on the  $XY$  plane. The  $xyz$  system is the principal axis system fixed in the body. The orbit plane is inclined to the  $XY$  plane by angle  $I$ ,  $\Omega$  is the longitude of the ascending node of the orbit plane on the  $XY$  plane measured from the inertial  $X$  axis along the direction to the vernal equinox,  $\mathbf{e}_o = \mathbf{e}_{Z'}$  is the orbit normal,  $\mathbf{e}_s = \mathbf{e}_z$  is a unit vector along the spin axis,  $\Omega_E$  is the longitude of the ascending node of Mercury's equator on the orbit plane relative to the  $X'$  axis,  $i$  is inclination of the equator plane relative to the orbit plane (obliquity),  $\psi$  is the angle between the ascending node of the equator and the  $x$  principal axis,  $\mathbf{r}$  points toward the Sun in the orbit plane and  $\omega$  and  $f$  are the argument of perihelion and true anomaly locating the Sun in the orbit plane relative to the  $X'$  axis.

In Peale (2005) it is shown that although the actual spin precession trajectory is slightly elliptical and the rate of precession is not quite uniform, a good approximation for the time variation of the spin vector is given by

$$\frac{d\mathbf{e}_s}{dt} = K_1 \cos i (\mathbf{e}_s \times \mathbf{e}_o) = -K_1 \cos i \sin i (\cos \Omega_E \mathbf{e}_{X'} + \sin \Omega_E \mathbf{e}_{Y'}) \quad (4)$$

where

$$K_1 = \frac{n^2 MR^2}{C\dot{\psi}} \left[ \frac{3}{2} J_2 G_{210}(e) + 3C_{22} G_{201}(e) \right] = K f(e), \quad (5)$$

with  $K = nMR^2 J_2/C$  and  $f(e) = G_{210}(e) + 2C_{22} G_{201}(e)/J_2$ , (used in Eq. (2)) and with  $\dot{\psi} = 3n/2$  being assumed. Eq. (4) follows from the average of the equations of motion over the orbit period as mentioned above with  $\dot{\psi} = 1.5n$ , and neglect of terms with coefficients that are small compared with Eq. (5). We can consider only the variation of the unit vector  $\mathbf{e}_s$  because  $\dot{\psi} \equiv 1.5n$  from the spin orbit resonance if we neglect the small physical librations. Eq. (4) shows the expected regression of the spin vector about the orbit normal. It is easiest to determine the equations of motion of the spin in the orbit frame of reference starting from

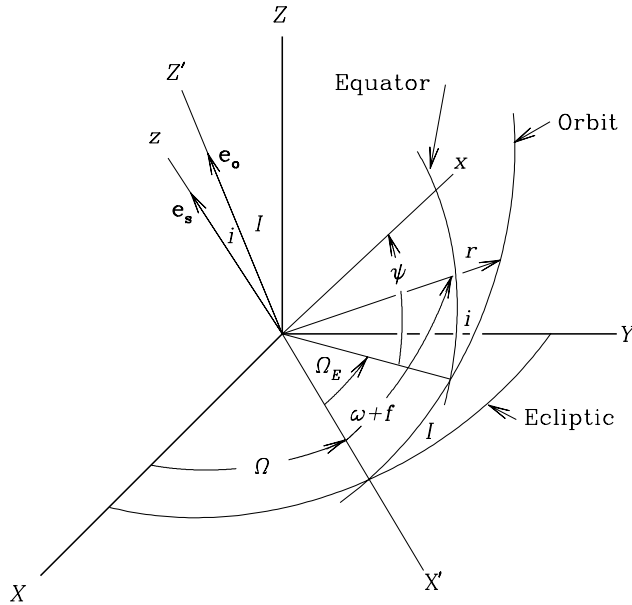


Fig. 2.— Coordinate systems used in determining time variation of Mercury’s spin vector, where  $\mathbf{e}_s$  and  $\mathbf{e}_o$  are unit vectors along the spin axis and orbit normal respectively. The  $XY$  inertial plane is the ecliptic plane of J2000.

the relation

$$\frac{d\mathbf{e}_s}{dt}_{inertial} = \frac{d\mathbf{e}_s}{dt}_{orbit} + \vec{w} \times \mathbf{e}_s = K_1 \cos i (\mathbf{e}_s \times \mathbf{e}_o), \quad (6)$$

where  $\mathbf{e}_s = \sin i \sin \Omega_E \mathbf{e}_{X'} - \sin i \cos \Omega_E \mathbf{e}_{Y'} + \cos i \mathbf{e}_{Z'}$  and  $\mathbf{e}_o = \mathbf{e}_{Z'}$  are defined in Fig. 2. The  $\mathbf{e}_i$  are unit vectors along the respective axes.

The angular velocity  $\vec{w}$  is nominally  $\vec{w}_L$ , the angular velocity of the orbit normal about the Laplace plane normal, but we can make another choice that simplifies the equations. The precession of the orbit normal about the Laplace plane normal leads to a velocity of the orbit normal  $\mathbf{e}_o$  of  $\vec{v} = \vec{w}_L \times \mathbf{e}_o$ , where  $\vec{w}_L$  is the angular velocity of the orbit normal parallel to the Laplace plane normal. Differentiation of the components of  $\mathbf{e}_o$  in the ecliptic frame yields components of  $\vec{v}$  that can be set equal to the like components of the cross product. However, these equations for the components of  $\vec{w}_L$  are not linearly independent, so one can only solve for two of the components in terms of the other, which serves as a free parameter. A convenient choice of the free parameter is the  $Z$  component of  $\vec{w}$ , where we have abandoned

the subscript, since another constraint is necessary to determine the Laplace plane normal.

$$\vec{w} = \left[ \frac{dI}{dt} \cos \Omega + \left( w_z - \frac{d\Omega}{dt} \right) \tan I \sin \Omega \right] \mathbf{e}_x + \left[ \frac{dI}{dt} \sin \Omega + \left( -w_z + \frac{d\Omega}{dt} \right) \tan I \cos \Omega \right] \mathbf{e}_y + w_z \mathbf{e}_z. \quad (7)$$

All of the solutions for  $\vec{w}$  lie in the plane determined by the orbit normal and the Laplace plane normal, where the latter is one of the set. The coplanarity is understood since all the  $\vec{w} \times \mathbf{e}_o$  must produce the same  $\vec{v}$ . If  $I'$  is the angle between  $\mathbf{e}_o$  and  $\vec{w}$ ,  $v = w \sin I'$  is a constant, and the magnitude  $w$  must decrease as  $I'$  increases. Eq. (7) is Eq. (13) of Yseboodt and Margot (2005), where they determine  $\vec{w}_L$  at a given epoch by adding the numerically determined constraint that the variation in the inclination  $I'$  is minimized in a 2000 year window centered on the epoch for data obtained from the 20,000 year JPL Ephemeris DE 408. At the epoch J2000, the ecliptic latitude and longitude of  $\vec{w}_L$  are  $86.725^\circ$  and  $66.6^\circ$  respectively corresponding to  $w_z = -1.91 \times 10^{-5}$  radians/year,  $I' = 8.6^\circ$  and an instantaneous precession period of 328,000 years. There is some uncertainty in these values from the statistical nature of the minimization process, but we shall see below that the uncertainty in the Laplace plane normal does not compromise the determination of the Cassini state.

The simplest form for  $\vec{w}$  in Eq. (7) is for  $w_z = d\Omega/dt$ . Since any choice of  $w_z$  in Eq. (7) yields the correct instantaneous motion of  $\mathbf{e}_o$ , we can use this simplest form,

$$\vec{w} = \frac{dI}{dt} \mathbf{e}_{x'} + \sin I \frac{d\Omega}{dt} \mathbf{e}_{y'} + \cos I \frac{d\Omega}{dt} \mathbf{e}_{z'}, \quad (8)$$

in Eq. (6) to determine the equations of motion of the spin in the orbit frame of reference. This choice of  $w$ , expressed here in the orbit frame, is just the vector sum of  $\overline{dI/dt}$  and  $\overline{d\Omega/dt}$  (Fig. 3). Equating like components in Eq. (6) yields three linearly dependent equations that can be solved uniquely for  $di/dt$  and  $d\Omega_E/dt$ . There results

$$\begin{aligned} \frac{di}{dt} &= -\sin I \sin \Omega_E \frac{d\Omega}{dt} - \cos \Omega_E \frac{dI}{dt} \\ \frac{d\Omega_E}{dt} &= -K_1 \cos i + \frac{\cos i \sin \Omega_E}{\sin i} \frac{dI}{dt} \\ &\quad - \frac{\cos i \cos \Omega_E \sin I + \sin i \cos I}{\sin i} \frac{d\Omega}{dt}, \end{aligned} \quad (9)$$

where  $dI/dt$  and  $d\Omega/dt$  are assumed known.

As expected,  $di/dt = 0$  and  $d\Omega_E/dt = -K_1 \cos i = \text{constant}$  if  $dI/dt$  and  $d\Omega_L/dt$  are both zero. If  $dI/dt = 0$  but  $d\Omega/dt$  is a negative constant, the equations describe the motion of the spin precession about a Cassini state in a uniformly precessing orbit. The Cassini state is displaced from the orbit normal in the plane defined by the orbit normal  $\mathbf{e}_o$  and the normal  $\mathbf{e}_L = -\vec{w}_L/w_L$  (Fig. 1) (Colombo 1966, Peale, 1969). This is the same plane containing all of the vectors defined by Eq. (7).



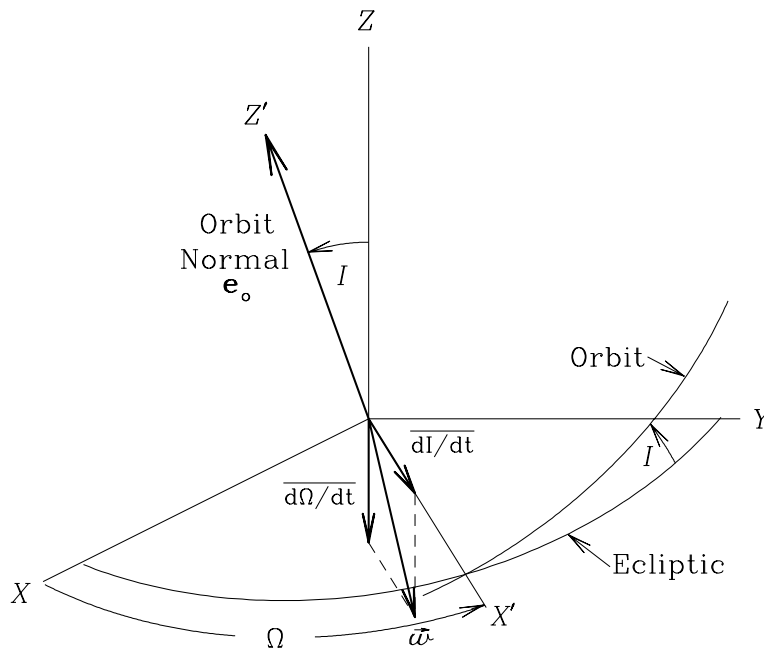


Fig. 3.— The vector sum of  $\overline{d\Omega/dt}$  and  $\overline{dI/dt}$  yields an effective precessional angular velocity  $\vec{\omega}$  of the orbit normal, which is the simplest choice from Eq. (7).

To eliminate the  $\sin i$  singularity in Eqs. (9) we introduce the variables  $p = \sin i \sin \Omega_E$  and  $q = \sin i \cos \Omega_E$ , with the result

$$\begin{aligned} \frac{dp}{dt} &= -K f(e) q \sqrt{1 - p^2 - q^2} - (\sin I \sqrt{1 - p^2 - q^2} + q \cos I) \frac{d\Omega}{dt}, \\ \frac{dq}{dt} &= K f(e) p \sqrt{1 - p^2 - q^2} - \sqrt{1 - p^2 - q^2} \frac{dI}{dt} + p \cos I \frac{d\Omega}{dt}. \end{aligned} \quad (10)$$

The numerical solution of Eqs. (10) yields the position of the spin vector of Mercury in the  $X'Y'Z'$  orbit system when all of  $e$ ,  $I$  and  $\Omega$  are varying.

### 3. Cassini state position

We wish to start the spin axis either in the initial Cassini state or close to it and determine how close it remains to the changing position of the state as the spin varies according to Eqs.

(10). From Eq. (12) of Peale (1974), the position of the Cassini state 1 is defined by

$$\begin{aligned} \sqrt{1 - e_{cz'}^2} \cos I' + e_{cz'} \sin I' - 2R' e_{cz'} \sqrt{1 - e_{cz'}^2} - 2S(1 + e_{cz'}) \sqrt{1 - e_{cz'}^2} &= 0 \\ e_{cz'} &= 0, \end{aligned} \quad (11)$$

where

$$\begin{aligned} R' &= \frac{3}{4} \frac{MR^2}{C} \frac{n^2}{\dot{\psi} w_L} J_2 G_{210}(e), \\ S &= \frac{3}{4} \frac{MR^2}{C} \frac{n^2}{\dot{\psi} w_L} C_{22} G_{201}(e), \end{aligned} \quad (12)$$

with  $e_{cx',y',z'}$  being the components in the orbit system ( $X'Y'Z'$ ) of  $\mathbf{e}_c$ , the unit vector along the Cassini state. For Mercury, Cassini state 1 is very close to the orbit normal (*e.g.*, Peale, 1969, 1974), which geometry is shown in Fig. 1. We can then set  $\sqrt{1 - e_{cz'}^2} = |\sin i_c| \approx i_c$ ,  $e_{cz'} \approx 1$  to first order in  $i_c$  and write

$$i_c = \frac{w \sin I'}{w(2R' + 4S - \cos I')}, \quad (13)$$

where we have replaced  $w_L$  by  $w = \sqrt{(dI/dt)^2 + (d\Omega/dt)^2}$ , the magnitude of the vector defined in Eq. (8) and used in the equations of motion of the spin. The inclination  $I'$  in Eq. (13) defined below is distinct for each choice of  $w$ . But since we have shown above that  $w \sin I'$  has the same value for all the values of  $w$  compatible with Eq. (7), the only change remaining after this substitution is the change in the term  $w \cos I'$  in the denominator. We shall see below that  $2R' + 4S \gtrsim 250 \gg \cos I'$ , so there is less than  $\sim 0.1\%$  change in  $i_c$ , ( $\approx 0.05''$  at the current epoch) effected by this substitution. Like the equations of motion for the spin (Eqs. (10)), use of this  $w$  in place of  $w_L$  greatly simplifies the numerical determination of the Cassini state position.

The inclination of the orbit  $I'$  to use in Eq. (13) is defined by

$$\frac{-(\mathbf{e}_o \cdot \vec{w})}{w} = \frac{\cos I}{\sqrt{1 + (dI/dt)^2 / (d\Omega/dt)^2}} = \cos I', \quad (14)$$

where the minus sign on the left hand side defines  $I'$  as a small positive angle when  $d\Omega/dt < 0$ . Eq. (13) thus defines the obliquity of the Cassini state in the orbit frame of reference for the values of  $e$ ,  $I$ ,  $dI/dt$  and  $d\Omega/dt$  at a particular time. As noted above, the Cassini state is in the plane defined by  $\mathbf{e}_o = \mathbf{e}_{z'}$  and  $\vec{w}$ , which plane also contains  $\vec{w}_L$ .

Using Eq. (8), we can write (Fig. 2)

$$-\vec{w} \times \mathbf{e}_o = -\frac{d\Omega}{dt} \sin I \mathbf{e}_{x'} + \frac{dI}{dt} \mathbf{e}_{y'} \quad (15)$$

to define the components of a vector in the orbit ( $X'Y'Z'$ ) system that is perpendicular to the plane containing the instantaneous Cassini state 1 and  $\vec{w}$  appropriate to the instantaneous

position of the latter vector. We already have the obliquity of the Cassini state from Eq. (13), so a unit vector along the instantaneous Cassini state in the  $X'Y'Z'$  system is

$$\mathbf{e}_c = \sin i_c \sin \Omega_c \mathbf{e}_{X'} - \sin i_c \cos \Omega_c \mathbf{e}_{Y'} + \cos i_c \mathbf{e}_{Z'}, \quad (16)$$

where

$$\begin{aligned} \cos \Omega_c &= \frac{-(d\Omega/dt) \sin I}{\sqrt{(d\Omega/dt)^2 \sin^2 I + (dI/dt)^2}}, \\ \sin \Omega_c &= \frac{dI/dt}{\sqrt{(d\Omega/dt)^2 \sin^2 I + (dI/dt)^2}}, \end{aligned} \quad (17)$$

with  $\Omega_c$  being the angle between the  $X'$  axis and the vector in the  $X'Y'$  plane defined by Eq. (15).

#### 4. Results for slow variations

We are now in a position to check just how well the adiabatic invariant is satisfied, or more directly, how well the spin follows the Cassini state. In Fig. 4 the variations of Mercury's eccentricity and inclination to the ecliptic of J2000 are shown for the last  $3 \times 10^6$  years from the data kindly provided by T. Quinn (Quinn, et al. 1991, See footnote <sup>1</sup>). These data have been filtered to exclude any terms with periods less than 2000 years. The justification for this filtering is that such terms usually are small amplitude oscillations that average to yield negligible contributions to the element variations. Note that keeping only contributions from terms with periods longer than 2000 years excludes any terms close to the spin precession period of between 1000 and 1100 years. The consequences of near resonant terms are discussed in Section 5. For the integrations, we divide Eqs. (10) by  $K$ , defined after Eq. (5), such that  $Kt$  is a dimensionless time. The period  $2\pi/K \approx 1365$  years would be close to the spin precession period for small  $e$  if  $C_{22} = 0$ . The dimensionless equations that are integrated are then Eqs. (10) with  $K$  removed from the coefficient of the first term on the rhs of the equations, and  $Kt \rightarrow t$ .

We note that the spin vector

$$\begin{aligned} \mathbf{e}_s &= \sin i \sin \Omega_E \mathbf{e}_{X'} - \sin i \cos \Omega_E \mathbf{e}_{Y'} + \cos i \mathbf{e}_{Z'}, \\ &= p \mathbf{e}_{X'} - q \mathbf{e}_{Y'} + \sqrt{1 - p^2 - q^2} \mathbf{e}_{Z'}, \end{aligned} \quad (18)$$

and that Eq. (16) can be written similarly with  $p$  and  $q$  replaced by  $p_c = \sin i_c \sin \Omega_c$  and  $q_c = \sin i_c \cos \Omega_c$  with  $i_c$  and  $\Omega_c$  being defined in Eqs. (13) and (17) respectively. We wish to determine the angle  $\delta$  between  $\mathbf{e}_s$  and  $\mathbf{e}_c$  as a function of time, where

$$\cos \delta = \mathbf{e}_s \cdot \mathbf{e}_c \approx 1 - \frac{\delta^2}{2}, \quad (19)$$

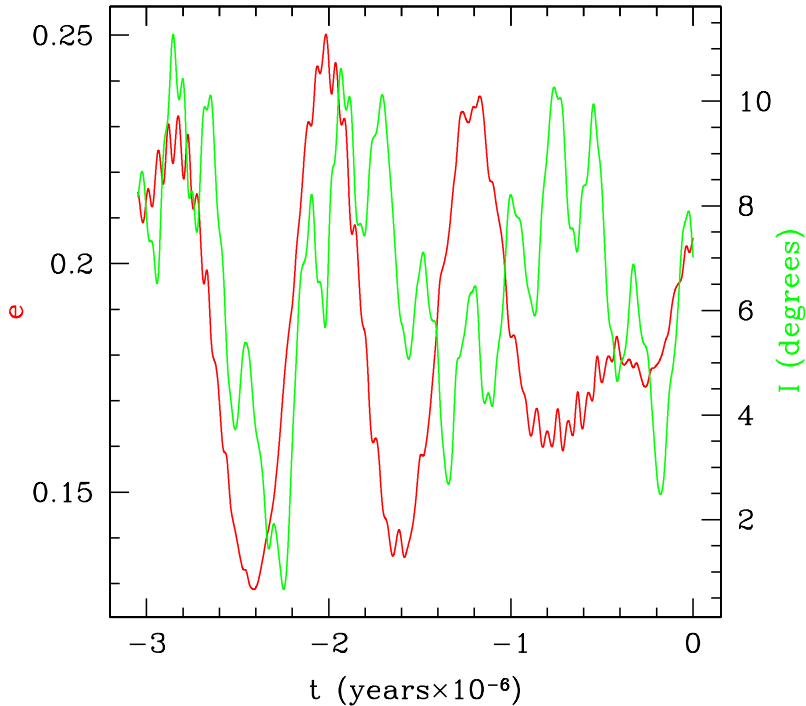


Fig. 4.— Variation of Mercury’s eccentricity and orbital inclination to the ecliptic of J2000 from T. Quinn (<ftp://ftp.astro.washington.edu/pub/hpcc/QTD>).

so that

$$\delta \approx \sqrt{p^2 + q^2 + p_c^2 + q_c^2 - 2pp_c - 2qq_c} \quad (20)$$

gives a more accurate value for  $\delta$  than numerically calculating  $\cos^{-1} \delta$  when  $\delta$  is very small. A cubic spline (Press et al. 1986) through the Quinn data points is used to determine  $e(t)$ ,  $I(t)$ ,  $\Omega$ ,  $dI/dt$  and  $d\Omega/dt$  in the calculation. The fact that contributions to the Quinn data with periods less than 2000 years have been eliminated, means the values of the variables can be used directly in calculating the position of the Cassini state without additional averaging (See Section 5). With the exception of the starting and ending values used to evaluate the second derivatives in the spline fit, the values of  $dI/dt$  and  $d\Omega/dt$  are determined as defined in the spline algorithm.

We show in Fig. 5 the trajectories of the projections of the unit spin vector  $\mathbf{e}_s$  and the unit vector in the direction of the Cassini state  $\mathbf{e}_c$  on the orbit plane over the  $3 \times 10^6$  year interval covered by the Quinn data. Initially, the two unit vectors are coincident ( $\delta(t = 0) = \delta_0 = \cos^{-1}(\mathbf{e}_s \cdot \mathbf{e}_c) = 0$ ). That the two trajectories are almost indistinguishable throughout the time interval shows how well the spin axis follows the Cassini state for variations in the parameters

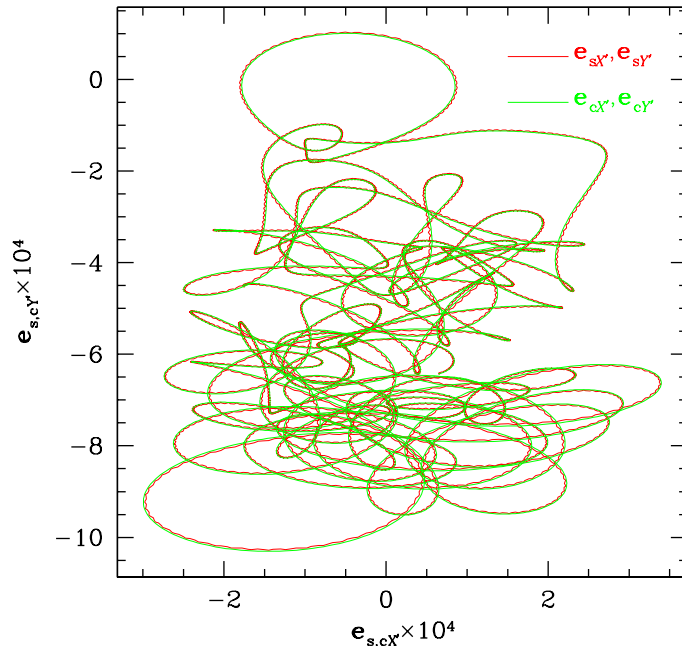


Fig. 5.— Trajectories of the projections of the unit spin vector  $\mathbf{e}_s$  and the unit vector in the Cassini state direction  $\mathbf{e}_c$  on the orbit  $X'Y'$  plane for variations in  $e$ ,  $I$ ,  $\Omega$ ,  $dI/dt$  and  $d\Omega/dt$  according to  $3 \times 10^6$  year simulations by T. Quinn.

that define the state. More precisely, we show in Fig. 6 the actual variations in  $\delta(t)$  for initial angular separations of  $0''$  and  $10''$ . The results for panel *a* were obtained with spline fits through all 6185 data points from the Quinn simulation, from which  $e(t)$ ,  $I(t)$ ,  $\Omega(t)$   $dI(t)/dt$  and  $d\Omega(t)/dt$  were determined at each call to the Bulirsch-Stoer integrator and at points therein. For panel *b* a spline fit through only every other data point was used including the first and last point of the full data set. For the same initial conditions, the deviations of the spin axis from the Cassini state in panel *a* are more scattered than those in panel *b* and reach a maximum of  $2.8''$ , whereas the maximum deviation in panel *b* is only  $1.2''$ , which difference is explained as follows.

The interval between data points in the Quinn simulation is 180,000 Julian days or approximately 493 years. The shortest period covered in a Fast Fourier Transform (FFT) of the data is the Nyquist period of 986 years (e.g. Press et al. 1986), which is less than the 1000-1100 year spin precession period. Although the spectral power at periods less than 2000 years are suppressed by as much as 9 orders of magnitude in the Quinn data (Quinn et al. 1991), we show in Section 5 that the system is extremely sensitive to variations in the inclination at periods near the spin precession period, which period is included in the full data set. An FFT of  $dI/dt$  constructed from the spline fit to the full data set sampled every 200 years, with

either Hanning or Welch window functions, yields some power down to the 984 year Nyquist period, which includes the precession period.

If we select only every other data point from the simulation, the Nyquist period is increased to 1972 years, which now excludes the resonant period. The FFTs of the spline fit and its derivative through the inclination points of the half data set sampled at 200 years reproduces the spectral power distribution of the full data set, but drops by more than two orders of magnitude for periods shorter than the 1972 year Nyquist period of the half data set. In other words, the half data set contains more than 100 times less power at the resonant period than the full data set, and this accounts for the more erratic behavior and larger maximum separation in panel *a*. We show in Section 5 that there is little or no spectral power near a period of 1000 to 1100 years in the full Mercury ephemeris. So the separations of the spin from the Cassini state indicated in panel *b*, where the spin is initially in the Cassini state, is more representative of the true limits on this separation as the orbital elements vary according to the Quinn solar system simulation over the 3 million year interval. Panel *c* shows that the spin remains within about 1'' of an initial separation of 10'' indicating that the adiabatic invariant is reasonably well preserved.

The source of the maximum separation of the spin from the Cassini state in panel *b* of Fig. 6 can be inferred by holding  $d\Omega/dt$  constant with precession period of 300,000 years and varying  $I$  and  $e$  according to

$$\begin{aligned} I &= I_0 + A_I \sin\left(\frac{2\pi t}{P_I}\right), \\ e &= e_0 + A_e \sin\left(\frac{2\pi t}{P_e} + \phi\right), \end{aligned} \tag{21}$$

and use the Quinn data to assign mean values  $I_0 = 6.0^\circ$ ,  $e_0 = 0.19$  and the following amplitudes with associated periods:

$$\begin{aligned} A_I &= 5.5^\circ \quad \text{for } P_I = 1 \times 10^6 \text{ yr}, \\ A_I &= 1.5^\circ \quad \text{for } P_I = 2 \times 10^5 \text{ yr}, \\ A_I &= 0.6^\circ \quad \text{for } P_I = 5 \times 10^4 \text{ yr}, \\ A_e &= 0.06 \quad \text{for } P_e = 8 \times 10^5 \text{ yr}, \\ A_e &= 0.01 \quad \text{for } P_e = 5 \times 10^4 \text{ yr}. \end{aligned} \tag{22}$$

Fig. 7 shows the results for  $\delta(t)$  for  $e$  and  $I$  variations with several combinations of the above amplitudes and periods. The initial value  $\delta_0 = 0$  is chosen for all cases. The large amplitude, long period variations lead to maximum deviations of the spin from the Cassini state of about 0.25'', whereas shorter period variations ( $P = 5 \times 10^4$  yr) with smaller amplitude lead to a maximum deviation a little more than 1''. It is these shorter period variations in the

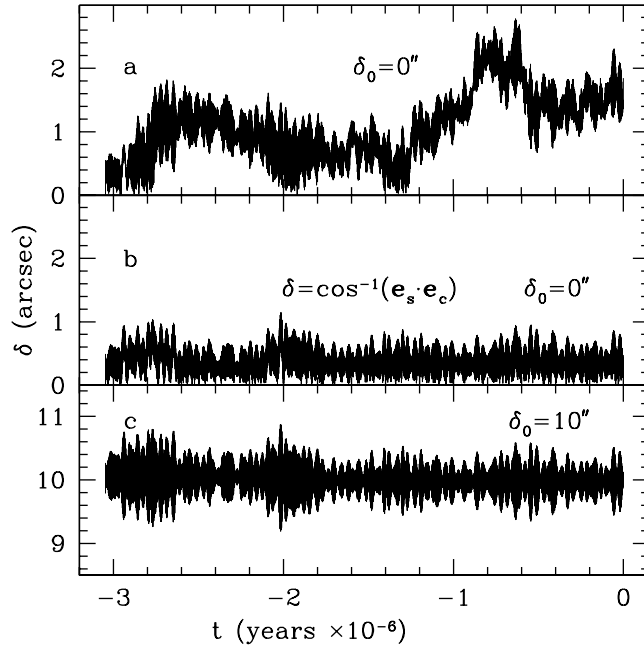


Fig. 6.— Separation  $\delta$  of the spin vector from Cassini state 1 for variations in  $e$ ,  $I$ ,  $dI/dt$  and  $d\Omega/dt$  from a simulation by T. Quinn. The spin is initially at the Cassini state in panels  $a$  and  $b$  and separated initially by  $10''$  in panel  $c$ . The separation  $\delta(t)$  in  $a$  is constructed from a spline fit through all 6185 data points in the Quinn simulation, whereas that in  $b$  results from a spline fit through every other point or 3093 points total. The reason for the differences in  $a$  and  $b$  is discussed in the text. Panel  $c$  shows the constancy of  $\delta$  to within  $\pm 1''$  for an initial value of  $10''$ .

the orbital parameters that are causing the maximum deviations of the spin from the Cassini state in Fig. 6. The fact that different values of  $A_e$  with  $P_e = 5 \times 10^4$  yr in combination with  $A_I = 1.5^\circ$  with  $P_I = 2 \times 10^5$  yr yield comparable maximum values of  $\delta(t)$  shows that variations in  $I$  are much more important than the variations in  $e$  in causing  $\mathbf{e}_s$  to not follow the Cassini state. Next, the maximum deviation from the Cassini state is almost proportional to  $A_I$  for a fixed  $P_I$ , from which we infer that it is really the maximum  $dI/dt$  that determines how much  $\mathbf{e}_s$  deviates from  $\mathbf{e}_c$ . If we set  $I = I_0 + (dI/dt)_{max}t$ , with  $(dI/dt)_{max} = 1.2 \times 10^{-4} \text{ }^\circ/\text{yr}$  from the spline fit to the Quinn data, the excursions of the spin away from the Cassini state over approximately  $3.5 \times 10^5$  years are shown in Fig. 8. For  $e \equiv 0.19$ , the maximum  $\delta < 0.6''$ . Imposing a periodic variation in  $e$  at the maximum amplitude of 0.06 while  $I$  is increasing linearly, induces a modulation in the maximum  $\delta$ , whose peaks approach only to  $0.8''$ .

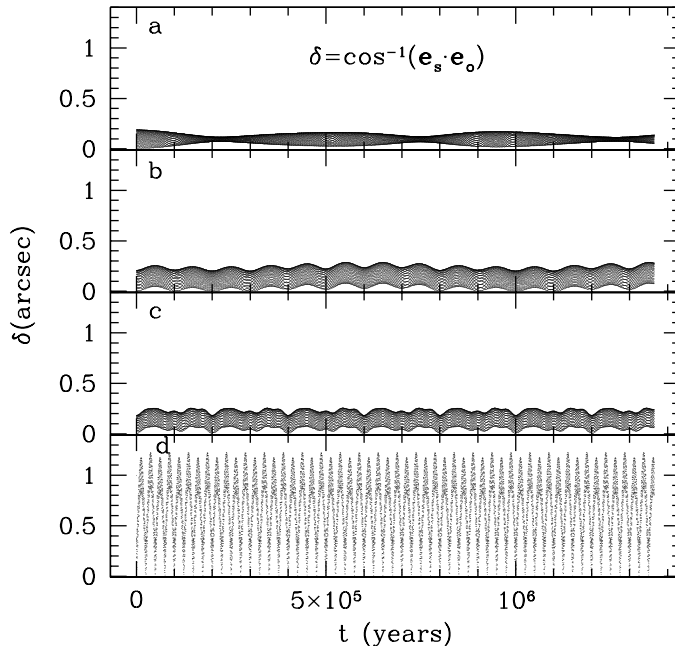


Fig. 7.— Separation of spin and Cassini state for periodic variations  $I = I_0 + A_I \sin(2\pi t/P_I)$ ,  $e = e_0 + A_e \sin(2\pi t/P_e + \phi)$ , where initially the spin axis and Cassini state are coincident. The amplitudes and periods are characteristic of those in the Quinn data.  $I_0 = 6.0^\circ$  and  $e_0 = 0.19$  are the real approximate mean values. These mean values and  $\phi = 0$  are assumed for all the cases. a)  $A_I = 5.5^\circ$ ,  $P_I = 10^6$  yr,  $A_e = 0.06$ ,  $P_e = 8 \times 10^5$  yr; b)  $A_I = 1.5^\circ$ ,  $P_I = 2.0 \times 10^5$  yr,  $A_e = 0.06$ ,  $P_e = 8 \times 10^5$  yr; c)  $A_I = 1.5^\circ$ ,  $P_I = 2 \times 10^5$  yr,  $A_e = 0.01$ ,  $P_e = 5 \times 10^4$  yr; d)  $A_I = 0.6^\circ$ ,  $P_I = 5 \times 10^4$  yr,  $A_e = 0.01$ ,  $P_e = 5 \times 10^4$  yr.

## 5. Results for short period variations

The Quinn data has been filtered to eliminate all variations with periods less than 2000 years, so it is instructive to look at the response of the system to short period fluctuations. For this purpose we use the complete Mercury orbital element variations, sampled every 500 Julian days from the JPL Ephemeris DE 408, that were kindly provided by Myles Standish. First we determine the location of the current Cassini state. Fig. 9 shows the variation over 20,000 years of  $e$ ,  $I$  and  $\Omega$  relative to the ecliptic plane, of J2000, where  $\Omega$  is measured from the vernal equinox. The variations are dominated by nearly linear secular changes with short period fluctuations superposed whose amplitudes are within the line widths of the curves. The current position of the Cassini state is necessary for the interpretation of the radar and future spacecraft information. We can determine a preliminary position of the Cassini state that will be refined when the MESSENGER spacecraft orbits Mercury. The



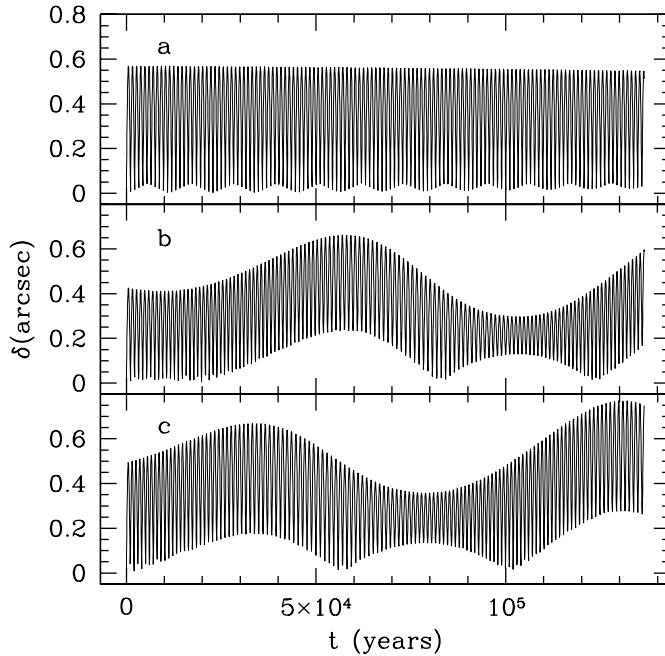


Fig. 8.— Separation of spin and Cassini state for the maximum  $dI/dt$  in the spline fit to the Quinn data.  $I = 7.35^\circ + (1.2 \times 10^{-4}/\text{yr})t$ . a)  $e = 0.19$ . b)  $e = 0.19 + 0.06 \sin 2\pi t/10^5 \text{yr}$ . c)  $e = 0.19 + 0.06 \sin [2\pi t/10^5 \text{yr} + 90^\circ]$

obliquity of the state is given by Eq. (13). For the value of  $w$  chosen for the equations of motion determinations, the precession period would be 286,660 years and  $I' = 7.51^\circ$ , whereas for the real value of  $w = w_L$  relative to the Laplace plane normal, the precession period would be 328,000 years and  $I' = 8.6^\circ$  (Yseboodt and Margot, 2005). Both sets yield  $w \sin I' = 1.641 \times 10^{-4} \text{ }^\circ/\text{year}$  in the numerator of Eq. (13). With  $C/MR^2 = 0.34$ , a central value of a plausible range (Harder and Schubert, 2001),  $e = 0.206$ ,  $n = 2\pi/(87.969 \text{ d})$ , 365.2563 d/y,  $(J_2, C_{22}) = (6.0 \times 10^{-5}, 1.0 \times 10^{-5})$  (Anderson *et al.* 1987),  $wR' = 0.1408^\circ/\text{year}$  and  $wS = 0.01437^\circ/\text{year}$  (Recall  $R'$  and  $S$  have  $w$  in their denominators.), the two choices of  $w$  and corresponding  $I'$  yield  $i_c = 1.6704'$  and  $1.6696'$  respectively, a difference of only  $0.05''$ , which justifies the use of  $w$  in place of  $w_L$  in the determinations of the Cassini state. Yseboodt and Margot (2005) find  $i_c = 1.68'$ . If we use the published uncertainties in  $J_2$  and  $C_{22}$  of  $\pm 2 \times 10^{-5}$  and  $\pm 0.5 \times 10^{-5}$  respectively and assume that the uncertainties in the ephemerides used to determine  $I'$  and the uncertainty in  $C/MR^2$  are negligible,  $1.18 < i_c < 2.51$  arcmin.

The unit vector corresponding to the Cassini state position  $\mathbf{e}_c$  is in the plane determined by the orbit normal  $\mathbf{e}_o$  and the  $\mathbf{e}_L$  on the opposite side of  $\mathbf{e}_o$  from  $\mathbf{e}_L$ . From the constraints that  $\mathbf{e}_c \cdot (\mathbf{e}_o \times \mathbf{e}_L) = 0$  and  $\mathbf{e}_c \cdot \mathbf{e}_o = \cos i_c$  and the unit magnitude of  $\mathbf{e}_c$ , three equations in the three components of  $\mathbf{e}_c$  can be solved for the current position of the Cassini state. It is

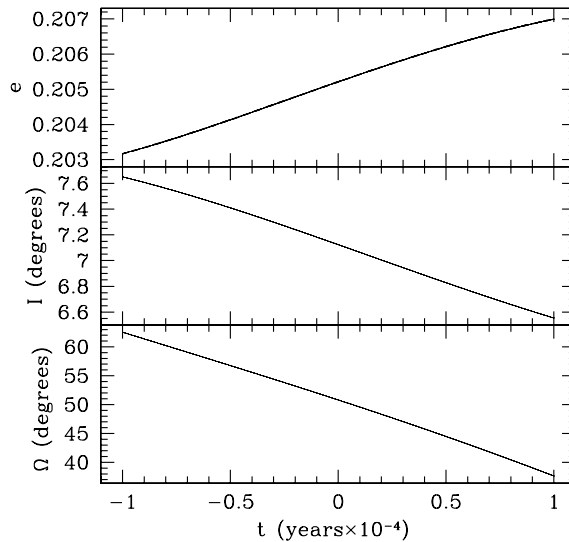


Fig. 9.— Variation of  $e$ ,  $I$  and  $\Omega$  relative to the ecliptic of J2000 for JPL Ephemeris DE 408.

less algebraically taxing to solve for the increments  $\Delta X$  and  $\Delta Y$  relative the projection of  $\mathbf{e}_o$  on the ecliptic plane to yield the ecliptic latitude and longitude of the Cassini state position of  $\lambda_c = 82.9694^\circ$  and  $\phi_c = -41.7585^\circ$  respectively for the J2000 epoch with  $i_c = 1.67'$ . The direction of the displacement is found from the intersection of the plane determined by  $\mathbf{e}_o$  and any of the  $\vec{w}$  from Eq. (7) and the unit sphere. This position will of course have to be adjusted as the uncertainties in the determining parameters are reduced.

The response of the angular separation  $\delta$  of spin axis  $\mathbf{e}_s$  and the Cassini state  $\mathbf{e}_c$  to short period fluctuations can be investigated by fixing  $e = 0.19$  and  $d\Omega/dt = -2\pi/(287,000 \text{ years})$  but forcing  $I$  to vary as  $I = I_0 + A_I \sin(2\pi t/P_I)$ . We fix the amplitude  $A_I$ , and determine the maximum separation of the spin from the Cassini state as a function of the period of the variation  $P_I$ . Panel *d* in Fig. 7 is characteristic of the behavior of the spin-Cassini state separation for periodic variations in  $e$  and  $I$ . The separation starting at  $\delta_0 = 0$  fluctuates between zero and a maximum, which is about  $1.2''$  in panel *d* in Fig. 7. Fig. 10 shows this maximum separation for periods ranging from 200 years to  $5 \times 10^4$  years for several values of  $A_I$ . Quite large separations of the spin from the Cassini state can result from such relatively short period oscillations in  $I$ , but most noticeably at periods near the period of the spin precession about the Cassini state, where a clear resonant response is evident.

We saw in Section 4 how a very small spectral power in the Quinn data at a period near the resonance more than doubled the maximum spin-Cassini state separation over the 3 million year interval from the  $1''$  maximum separation when spectral power at that period was suppressed by halving the number of data points. To check whether there is significant power

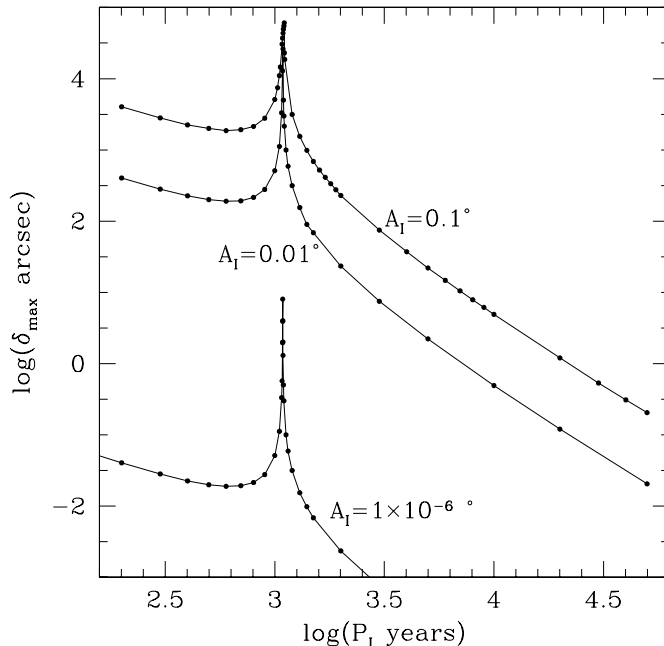


Fig. 10.— Maximum separation of the spin axis from the Cassini state for periodic variation of  $I$  with amplitude  $A_I$  with  $e = 0.19$  and  $d\Omega/dt = -2\pi/(287,000 \text{ years})$  as a function of the period of variation.

in the real variations in  $e$ ,  $I$ ,  $\Omega$ ,  $dI/dt$  and  $d\Omega/dt$  at the resonant period or at any other short period that could cause the spin to separate from the Cassini state by a large angle, we repeat the exercise in Section 4, but now with the variations in  $e$ ,  $I$  and  $\Omega$  and their derivatives given by the ephemeris DE 408. Fig. 9 shows that the short period fluctuations in  $e$ ,  $I$  and  $\Omega$  are small compared to significant almost linear variations.

As was done with the Quinn data, we represent the variations in  $e$ ,  $I$ , and  $\Omega$  with spline fits that capture the short period fluctuations in these elements as well as their derivatives derived therein for use in Eqs. (10). The Cassini state position is determined at arbitrary times from averaged values of the parameters, with  $\langle e \rangle$ ,  $\langle I \rangle$ , and  $\langle \Omega \rangle$  being averages determined by the sum of the values at the extremes of a 2000 year window centered on the epoch divided by 2, and  $\langle dI/dt \rangle$  and  $\langle d\Omega/dt \rangle$  are the difference in the values at the extremes divided by 2000 years.

In Fig. 11, the equivalent of Fig. 5 the projections of the components of  $\mathbf{e}_s$  and  $\mathbf{e}_c$  onto the orbit plane are shown over the 20,000 year interval of the ephemeris, where the projection of  $\mathbf{e}_c$  is truncated at the endpoints because of limits of the averaging process. Fig. 11 represents a short segment of one of the loops in Fig. 5 extended into the future to J10000, except now

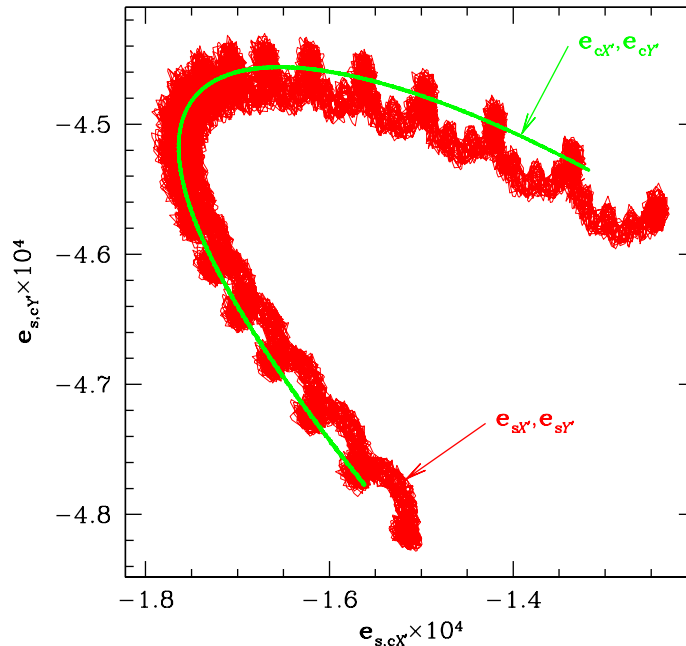


Fig. 11.— Trajectories of the projections of the unit spin vector  $\mathbf{e}_s$  and the unit vector in the Cassini state direction  $\mathbf{e}_c$  on the orbit  $X'Y'$  plane for variations in the orbital elements according to the 20000 year JPL Ephemeris DE 408.

all of the high frequency terms are included in the variations of  $e$ ,  $I$  and  $\Omega$  for the variation of the spin position. Again the spin is initially in the Cassini state ( $\delta_0 = 0$ ), and we see that it remains close to that state as we have defined it in terms of the averages of the ephemeris data. In Fig. 12, the equivalent of Fig. 6b, we show that the spin, initially in the Cassini state, stays within  $1''$  of the Cassini state over the 20,000 year interval of the ephemeris. There are no short period terms in the real variations of  $e$  and  $I$  that can lead to the large periodic separations shown in Fig. 10. In particular, there are no contributions to the variations that are near resonance with the spin precession, and the spin will remain close to the Cassini state for both long period and short period variations in the orbital elements and variations in the Laplace plane orientation that define the position of the state.

## 6. Discussion

We have shown that Mercury’s spin axis will stay within approximately  $1''$  of the time varying position of Cassini state 1 after dissipative processes have brought it to the state for both long and short period variations in the orbital parameters. Yseboodt and Margot (2005) also find

1

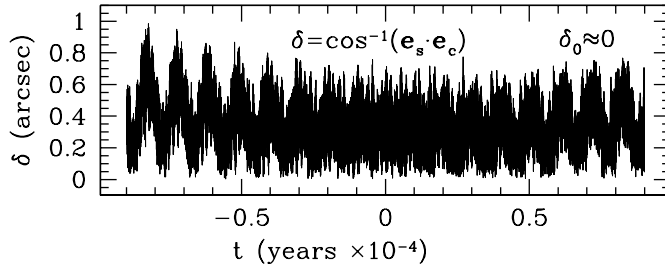


Fig. 12.— Separation  $\delta$  of the spin vector from Cassini state 1 for variations in  $e$ ,  $I$  and  $\Omega$  from JPL ephemeris DE 408 covering 20,000 years centered on calendar year 0 and sampled every 500 ephemeris days. The spin is initially at Cassini state 1 in this example, and the separation is deduced from a spline fit through the 14,624 data points of the ephemeris. The periodicity in  $\delta$  is that of the free precession of the spin about the Cassini state.

that Mercury’s spin axis remains close to the Cassini state as the position of the state is altered by slowly increasing the planetary masses from zero to their current values with time scales that are long compared to the spin precession period. The maximum separation of 1” that we found is about 1% of the 1.67’ current obliquity of the Cassini state. Current estimates for the precision of the MESSENGER spacecraft determination of Mercury’s obliquity are about 10% of its value (Zuber and Smith, 1997), although this precision may possibly be exceeded by radar measurements. In any case the maximum deviation of Mercury’s obliquity from the Cassini state obliquity induced by the slow and fast orbital variations and by the changing geometry of the solar system is sufficiently small that reasonably precise values of  $C/MR^2$  will be obtainable from the radar and spacecraft observations with correspondingly tight constraints on  $C_m/C$ . This conclusion depends of course on there being no recent excitation of a free spin precession. With tight constraints on both  $C/MR^2$  and  $C_m/C$ , the internal structure of Mercury should be reasonably well constrained.

For the small coupling that is likely between Mercury’s liquid core and solid mantle, the core is not likely to follow the mantle on the spin precession time scale as we have assumed here.

If the mantle precesses independently of the core, the polar moment of inertia for the spin precession will be about half of the total moment of inertia. The spin precession period will be 500 years instead of the 1000 years assumed here. The mantle would relax to a somewhat different Cassini state which would gradually relax to the current state as dissipative processes cause the liquid core to catch up on a time scale short compared to the 300,000 year orbit precession time scale. It may be the case that there is a slight offset of the spin axis from the Cassini state because of the fluid coupling between core and mantle. If this offset is measurable, it will provide a constraint on the core-mantle coupling. Investigation of this conjecture will be included in a following paper, where core and mantle are considered as independent but coupled entities.

## 7. Acknowledgements

It is a pleasure to thank Man Hoi Lee and Gerald Ramian for very helpful discussions and M. H. Lee for some informative numerical calculations. Critical reviews by Jean-Luc Margot and Jacques Henrard motivated changes in presentation that greatly improved the manuscript. Marie Yseboodt and Jean-Luc Margot pointed out a serious error introduced into the revised version of the manuscript. Thanks are also due Tom Quinn for providing the files from his 3 million year simulation of the solar system and Myles Standish for kindly providing Mercury's orbital variations in a convenient format from his just completed 20,000 year JPL DE 408 ephemeris. This work is supported in part by the Planetary Geology and Geophysics Program of NASA under grant NAG5 11666 and by the MESSENGER mission to Mercury.

## 8. References:

- Anderson, J.D., Colombo, G., Esposito, P.B., Lau, E.L., Trager, T.B. 1987. The mass, gravity field and ephemeris of Mercury. *Icarus* 71, 337-349.
- Anselmi, A., Scoon, G.E.N. 2001. BepiColombo, ESA's Mercury Cornerstone mission. *Planet. Space Sci.* 49, 1409-1420.
- Beletskii, V.V. (1972) Resonance rotation of celestial bodies and Cassini's laws. *Cel. Mech.* 6, 356-378.
- Colombo, G. (1966) Cassini's second and third laws, *Astron. J.* 71, 891-96.
- Goldreich, P., Toomre, A. 1969. Some remarks on polar wandering, *J. Geophys. Res.* 74, 2555-2567.

- Harder, H., Schubert, G. 2001. Sulfur in Mercury's core? *Icarus* 151, 118-122.
- Kaula, W.M. 1966 *Theory of satellite geodesy; applications of satellites to geodesy*, Blaisdell, Waltham, MA.
- Margot, J.L., Peale, S.J., Slade, M.A., Jurgens, R.F., Holin, I.V., 2003. Mercury interior properties from measurements of librations. Mercury, 25th meeting of the IAU, Joint Discussion 2, 16 July, 2003, Sydney, Australia, meeting abstract. (<http://adsabs.harvard.edu>).
- Peale, S.J. 1969. Generalized Cassini's laws, *Astron. J.* 74, 483-89.
- Peale, S.J. 1974. Possible histories of the obliquity of Mercury, *Astron. J.* 79, 722-44.
- Peale, S.J. 1976. Does Mercury have a Molten Core? *Nature* 262, 765-766.
- Peale, S.J. (1981) Measurement accuracies required for the determination of a Mercurian liquid core, *Icarus* **48**, 143-45.
- Peale, S.J. 1988. Rotational dynamics of Mercury and the state of its core, In Mercury, ed. F. Vilas, C.R. Chapman, M.S. Matthews, U. of Arizona Press, Tucson, 461-493.
- Peale, S.J. 2005. The free precession and libration of Mercury, *Icarus*, In press.
- Peale, S.J. Phillips, R.J., Solomon, S.C., Smith, D.E., Zuber, M.T., 2002. A procedure for determining the nature of Mercury's core, *Meteor. Planet. Sci.* 37, 1269-1283.
- Press, W.H., Flannery, B.P., Teukolsky, S.A., Vetterling, W.T. *Numerical Recipes* Cambridge University Press, London, p. 86.
- Quinn, T.R., Tremaine, S., Duncan, M. 1991. A three million year integration of the Earth's orbit, *Astron. J.* 101, 2287-2305.
- Solomon, S.C., 20 colleagues 2001. The MESSENGER mission to Mercury: Scientific objectives and implementation, *Planet. Space Sci.* 49, 1445-1465.
- Ward, W.M. 1975. Tidal friction and generalized Cassini's laws in the solar system, *Astron. J.* 80, 64-70.
- Yseboodt, M. and Margot, J.L. 2005. Evolution of Mercury's Obliquity, Submitted to *Icarus*.
- Zuber M. T. and Smith D. E. 1997. Remote sensing of planetary librations from gravity and topography data: Mercury simulation (abstract). *Lun. Planet. Sci.* **28**, 1637-1638.